dubey saket (Orcid ID: 0000-0001-9619-4185)
Goyal Manish, Kumar (Orcid ID: 0000-0001-9777-6128)

Glacial Lake Outburst Flood (GLOF) Hazard, Downstream Impact, and Risk over the Indian Himalayas

Authors: Saket Dubey, Manish Kumar Goyal

Indian Institute of Technology, Indore, India.

Corresponding author: Saket Dubey (saketdubey4@gmail.com)

Key Points:

- Avalanche trajectories suggest that 36 out of 329 glacial lakes are susceptible to dynamic failure via an avalanche entering the lake.
- Application of stochastic flood model reveals that 67 glacial lakes contain at least one hydropower system along their flow path.
- Indian Himalayas contain 23 critical glacial lakes, 17 of which are located in the state of Sikkim.

Abstract

Indian Himalayas are home to numerous glacial lakes, which can pose serious threat to downstream communities and lead to catastrophic socio-economic disasters in case of a glacial lake outburst flood (GLOF). This study first identified 329 glacial lakes of size greater than 0.05 km^2 in the Indian Himalayas and then a remote-sensing based hazard and risk assessment was performed on these lakes. Different factors such as avalanche, rockfall, upstream GLOF, lake expansion, identification of the presence of ice cores and assessment of the stability of moraine were considered for the hazard modelling. Further, a stochastic inundation model was applied to quantify the potential number of buildings, bridges and hydropower systems that could be inundated by GLOF in each lake. Finally, the hazard parameters and downstream impact were collectively considered to determine the risk linked with each lake. A total of 23 lakes were identified as very high-risk lakes and 50 as high-risk lakes. The potential flood volumes associated with various triggering mechanisms were also measured and were used to identify the lakes with the most considerable risk, such as Shakho Cho and Khangchung Tso. This study is anticipated to support stakeholders and decision-makers in identifying critical glacial lakes and make well-informed decisions related to future modelling efforts, field studies and risk mitigation measures.

Keywords: Glacial lakes; Glacial lake outburst flood; India; Avalanche; Sentinel

1 Introduction

The Himalayas have observed extensive shrinkage of glaciers with the most negative mass balance and the most significant decline in glacial length (Cogley, 2016; Gardelle et al., 2011; Kääb et al., 2012; Maurer et al., 2019; Sakai & Fujita, 2017; Yao et al., 2012). This glacial retreat is accompanied by the formation of numerous glacial lakes formed by replacing ice from glacier tongues (King et al., 2017, 2018). Linsbauer et al., (2016) predicted the future emergence of glacial lakes in Himalayas by modelling glacier bed topographies and documented 5000 overdeepenings that may turn into glacial lakes. Sporadic outbursts in the unstable glacial lake have killed thousands of people with some of the most significant events taking place in the Himalayas (Nie et al., 2018; Veh et al., 2018). Carrivick & Tweed, (2016) compiled an inventory of glacier floods and reported that the central Himalayas have observed maximum number of causalities due to glacial hazards, where Nepal and India have observed fewer flood but higher levels of damage. Glacial lake outburst flood (GLOF) is the sudden discharge of a large amount of stored water from glacial lakes (Carrivick & Rushmer, 2006), triggered majorly due to dynamic failure (mass entering the lake in the form of avalanche, rockfall or GLOF in the upstream portion of the lake) and minorly due to self-destructive failures (settlement of ice-cored moraine or unstable moraine structure), seismic activities, earthquake and extreme climatic events (Carrivick & Tweed, 2013; Rounce et al., 2016; Worni et al., 2013). The remote location, infrequent occurrence and interconnection between these triggering mechanisms makes it difficult to assess the potential hazard related to these lakes. Nonetheless, the estimated risk from various triggering mechanisms must be quantified, especially for the Himalayas, where 68% of the hydropower plants are located on potential GLOF tracks (Schwanghart et al., 2016).

Hindu Kush Himalayas have been subjected to many glacial lake studies (Adam Emmer, 2018; Fujita et al., 2013; Ives et al., 2010; King et al., 2017, 2018; Maharjan et al., 2018; Schwanghart et al., 2016; Veh et al., 2019), including the ones carried out for specific countries such as Nepal (Mool et al., 2011; Rounce et al., 2017; Somos-Valenzuela et al., 2015), Bhutan (Komori, 2008; Ukita et al., 2011) and Tibet (Chen et al., 2007; Cui et al., 2011; Wang et al., 2011). Studies carried out for the Indian Himalayas includes the work of ICIMOD (Ives et al., 2010) that created a comprehensive glacial lake inventory of Hindu Kush Himalayas and included three Indian states. Worni et al., (2013), created a glacial lake inventory for Indian Himalayas (>0.01 km^2) and carried out a detailed risk assessment. Indian Himalayas were also subjected to many regional studies focusing particularly on specific region or lake (Abdul Hakeem et al., 2018; Aggarwal et al., 2017; Raj et al., 2013; Sattar et al., 2019). Most of the above-mentioned studies were carried out using glacial lake data derived from medium resolution Landsat imageries, whereas, with the proliferation of satellite data, higher spatial resolution optical satellite data is available even at no-cost public domain such as Resourcesat-2 (RS-2) Linear Imaging Self Scanning (LISS-3) and Sentinel 2 multispectral instrument (MSI) dataset (Drusch et al., 2012).

Documentation of critical glacial lakes and application of remedial measures can prevent events such as the ones occurred at Ayaco Lake in 1969 and 1970 (Liu et al., 2013), Nare Lake in 1977 (Buchroithner et al., 1982), Dig Tsho in 1985 (Vuichard & Zimmermann, 1987), Sabai Tsho in 1998 (Osti & Egashira, 2009), and Chorabari in 2013 (Allen et al., 2016; Kanti et al., 2019); these events are the example of calamitous GLOF events that have caused extensive damage to lives and socioeconomic condition of inhabitants (Carrivick & Tweed, 2016). Assessment of glacial lake hazards have been performed using regional data at China (Chen et al., 2010), Nepal (Bajracharya & Mool, 2009; Mool et al., 2011), Bhutan (Nagai et al., 2017),

Tibet (Chen et al., 2010) and India (Worni et al., 2013). The major distinctions among these studies are the choice of parameters and the respective weights assigned to these parameters. The application of various parameters and weights leads to contradictory hazard classification (Emmer et al., 2016; Rounce et al., 2016) which can create confusion among stakeholders. Therefore, the objective of this study is to develop a novel framework to analyse the glacial lakes holistically, i.e., accounting for primary triggering mechanisms and framed with an objective approach to enable smooth decision making.

To the best of our knowledge, present investigation is the first to examine the hazard, downstream impact and risk of glacial hazard in a holistic manner accounting for both self-destructive and dynamic failure accompanied with the determination of downstream impact in terms of public utilities such as buildings, bridges and hydropower systems over the entire Indian Himalayas. Also, most of the earlier studies in the Indian Himalayas were based on self-destructive failures, however, to represent the complex mechanism of GLOF, more comprehensive framework that accounts for most frequent triggers is required.

2 Method

2.1 Glacial lake inventory

This study includes glacial lakes in the Indian Himalayas that are greater than 0.05 km^2 (Figure 1). The 0.05 km^2 threshold was applied to maximise the number of glacial lakes which is also consistent with past catastrophic GLOF events (Nie et al., 2018). Glacial lakes were delineated for the fall of 2018 using Sentinel-2 Multispectral Instrument (MSI) imageries and to assess the temporal change in lake dimensions the glacial lakes were delineated for the year 1993 using Landsat 5 Thematic Mapper Plus (TM) imageries. The presence of clouds hinders the visibility of imageries. Therefore, for the cloud masked lakes, the imageries of 2017 were used to assist the lake delineation of 2018 whereas imageries of 1992 were used to assist the lake delineation of 1993. The initial period for the lake delineation was considered to be 1992 as this year represents the initial stage of Landsat 5 data availability during the months of least snow cover for the Indian Himalayas. Glacial lake boundaries were manually delineated and the presence of glacial lake was identified using the Normalized Difference Water Index (NDWI; McFeeters, 1996). Uncertainty in lake delineation was presumed to be the lake perimeter multiplied by half the pixel size (Rounce et al., 2017; Shukla et al., 2018). Glacial lakes were categorised as moraine-dammed lake, ice-dammed lake, bedrock-dammed lake and other glacial lakes (Maharjan et al., 2018). Glacier outlines were obtained from Randolph Glacier Inventory Version 5.0 (RGI; Arendt et al., 2015), which is based on satellite imageries acquired between 1999 and 2003. The uncertainty associated with RGI inventory has been estimated to be ~15% (Nuimura et al., 2014).

2.2 Glacial hazard and downstream impact

Hazard assessment implies determination of susceptibility to various triggers such as avalanche, rockfall, upstream GLOF, lake expansion, presence of ice cores and instability of damming moraine. The present study aimed at modelling self-destructive failures using hydrostatic pressure, presence of ice-core in damming moraine and significant expansion over time. Whereas, dynamic failure (mass inflowing into the lake) using ice avalanche trajectories,

landslide/rockfall, and upstream GLOFs. The workflow of the presented methodology is depicted in Figure 2(a).

The combination of average steep lakefront area (SLA; Fujita et al., 2013) angle and the presence of ice-cored moraine was utilised to assess the moraine's stability. Steep lakefront area determines the lowering (H_p) of the glacial lake in case of a breach. A threshold of 10° on the SLA angle was applied based on the implementation of SLA concept on five previously outbursted glacial lakes by Fujita et al., (2013). Google Earth and Sentinel imageries were utilised to identify supraglacial ponds or change in the outlet channel to estimate the presence of ice core in the damming structure (Rounce et al., 2016; Watson et al., 2018). Though the bedrock dammed lakes will not produce a GLOF by dam failure but may produce a GLOF by overtopping, still to apply a standardized analysis, the SLA was determined for all the lakes irrespective of their dam type. Lakes were considered significantly expanded if the areal expansion of lake between 2018 and 1993 exceeded the errors associated with 1993 lake delineation.

Advanced Spaceborne Thermal Emission and Reflection Radiometer (ASTER) Global Digital Elevation Model Version 2 acquired between 2000 and 2010 with spatial resolution of 30 m and absolute vertical accuracy of ~17 meters (Tachikawa et al., 2011), hereon referred as DEM in conjunction with RGI was used to determine the areas that are prone to an avalanche, i.e., any glaciated region with slope ranging between 45-60° (Alean, 1985; Osti et al., 2011). Avalanche prone areas were then cumulated into maximum avalanche-prone areas using a variable kernel filter with 100 % threshold. Here, a 1×1 grid was checked, and if all the pixels were prone to an avalanche, it was expanded to a 2×2 pixel grid. This expansion of the grid was continued until it fails to meet the threshold of 100%. Furthermore, three scenarios were assumed considering the avalanche thicknesses of 10 m, 30 m and 50 m respectively; these thicknesses are consistent with their relationship between slope and shear stress and are of the same order as observed in Switzerland, Austria, and Alaska (Alean, 1985). These thicknesses were combined with the maximum avalanche-prone area to determine the avalanche volume. A minimum threshold of 0.1×10^6 m^3 was applied on lake volume as defined by Richardson & Reynolds, 2000, a volume large enough to destroy a village. Data on ice avalanche volume triggering a GLOF is scarce; However GLOF models attempting to model ice avalanche and wave propagation have found that an avalanche of 0.5×10^6 m^3 is required to trigger an outburst (Somos-Valenzuela et al., 2016; Worni et al., 2014). Avalanche volumes were then used to determine the average angle between the initial point of the avalanche to the last point based on the equation given by Huggel et al., (2004), i.e., Equation 1.

$$\tan(\alpha) = 1.11 - 0.118\log(V) \qquad \text{Equation 1}$$

where V and α denote the volume of avalanche (m^3) and the average slope trajectory (°) also referred to as "look-up" angle, respectively. The minimum threshold selected for the average look-up angle was 17° as avalanche rarely exceed this limit (Huggel et al., 2004). The avalanche trajectories were then estimated using a flow direction algorithm with the sink filled DEM up to the point where the average look-up angle was attained. Rockfalls were modelled similarly with rock thickness of 4 m and an average look-up angle of 20° (Collins & Jibson, 2015). Furthermore, area prone to a rockfall was assumed to be any non-glaciated region with its slope exceeding 30° (Bolch et al., 2011; Rounce et al., 2016). Sensitivity analysis was implemented by changing the average look-up angle by ±3°. Any GLOF event in the upstream

of glacial lake having the ability to cascade a series of GLOF events was modelled using Monte-Carlo least-cost path method (MC-LCP; Watson et al., 2015); MC-LCP uses Monte Carlo loop to model DEM uncertainty and implements an iterative least-cost path analysis to produce inundation probabilities for each DEM cell. This method is computationally inexpensive and relies merely on the geometry of the downstream channel acquired from the DEM. It generates the flow path without differentiating between flash floods and debris flows. As the model has no physical basis, the model was implemented considering the conservative flood extent generated when compared to the flood extent of 1985 GLOF of Dig Tsho (Watson et al., 2015) and due to limited data availability on previous GLOFs, against the flood extents of two-dimensional debris flood model FLO-2D for Lmja Tsho (Rounce et al., 2016) and HEC-RAS for South Lhonak Lake (Sattar et al., 2019), Sikkim (Supplementary Figure S1). MC-LCP model implemented with both Shuttle Radar Topography Mission (SRTM) DEM v.4 and Aster GDEM v.2 generated reasonable flood extent when compared against the flood extent generated by Sattar et al., 2019 except for few places, where the model does not capture the simulated flood extent. This could be highly problematic for downstream impact assessment if these areas were populated. More detailed analysis on the comparison of the flood extent from both the DEMs revealed that GDEM v 2.0 tracked the main channel better. Therefore, MC-LCP along with Aster GDEM v2 was used to model potential GLOF from each lake.

Each lake was assessed for its downstream impact using MC-LCP model with a cut off distance of 50 km to facilitate a standardized comparison between different lakes; the 50 km threshold was consistent with GLOF event at Dig Tsho in 1985 (Watson et al., 2015), Chilleon Valley in 2015 (Wilson et al., 2019), Chorabari in 2013 (Rafiq et al., 2019), etc. Although some of the GLOF events have shown runout length up to 200 km (Richardson & Reynolds, 2000), considering such outliers may lead to overestimation of downstream impact. Generated flood extents were used to assess the downstream impact of GLOF for each lake by quantifying the number of bridges, hydropower systems, and buildings that could be affected. The number of hydropower systems that could be affected was primarily assessed using the database available from forty-third report on hydropower by Ministry of India but it was later acknowledged that the available location of various hydropower systems was representative of the system but not essentially the location of a particular part of system such as dam. To resolve this discrepancy, hydropower systems were manually marked using Google Earth and Google Maps. The locations of the buildings were retrieved from OpenStreetMap (https://www.openstreetmap.org) and were confirmed and updated using Google earth. For the Indian Himalayas, the buildings were majorly underrepresented; more than 10000 buildings were updated for the local inventory. Bridges were identified using OpenStreetMap as any road crossing the watercourse.

The potential flood volume (PFV) for each lake was assessed by calculating the maximum PFV of self-destructive and dynamic failure. In case of self-destructive failure, the PFV was estimated using the approach from Fujita et al., (2013) but to determine the mean depth and lake volume, equation from Cook & Quincey, (2015) was utilised, (Equation 2 and 3)

$$D_m = 0.1217A^{0.4129} \quad \text{Equation 2}$$

$$V = 0.1217{A_l}^{1.4129} \quad \text{Equation 3}$$

where A_l is the lake area in 2018 (m^2), D_m is the mean depth (m) and V is the lake volume (m^3). These equations were used to limit the PFV to the maximum of lake volume. In case of dynamic failure, the PFV was estimated based on the assumption that the water displaced will be equal to the volume of mass entering the lake. These estimates of PFV have significant uncertainties that need to be taken into account and propagated to the final results; Schwanghart et al., (2016) used a stochastic approach to predict outburst flood volumes and estimated that peak discharge may vary up-to two order of magnitude for a given lake area. In this study, our aim was to provide a quantitative comparison of glacier flood risks rather than to precisely define the absolute flood of any individual flood event. Therefore, a simplistic sequential perturbation approach was used for PFV error estimation, where we evaluated PFV uncertainty ($dPFV$) using Equation 4, whereas importance of d_D (error in depth estimation) in estimated uncertainty using Equation 5

$$dPFV = \pm\sqrt{((A + d_A)D - AD)^2 + ((D + d_D)A - AD)^2} \quad \text{Equation 4}$$

$$Importance = \frac{((D+d_D)A-AD)^2}{dPFV^2} \quad \text{Equation 5}$$

Here d_A and d_D represents the errors in area and depth estimation, respectively. For the case where higher PFV is estimated using SLA analysis, the parameters D and A represent the lake mean depth and lake area, respectively. In this case, we computed the error in-depth estimation based on root mean square error (RMSE) of bathymetric derived depth for 42 glacial lakes (Cook & Quincey, 2015; Supplementary table sheet 9) against the mean depth obtained from equation 2 and computed the RMSE value to be 6.7 m. The error in area estimation was determined by multiplying the shoreline value with half the pixel size of Sentinel 2 MSI data (10 m). In the case, where PFV is found to be greater for avalanche (rockfall), D represent the mean depth of avalanche (rockfall) and A represent the maximum prone area for avalanche (rockfall). Due to scarce data availability on avalanche (rockfall) depth. Mean depth of avalanche (rockfall) was assumed to be 30 m (4m) with error in-depth estimation of 20 m (2 m); whereas, the error in area estimation was found to be 15%, based on the uncertainty associated with the glacier inventory (Nuimura et al., 2014).

2.3 Risk

The focal objective of the study was to assess the risk associated with each lake, which can be represented as a combined characteristic of hazard and downstream impact. The framework was adopted from Rounce et al., 2016 with slight variation to prioritise the lakes with the highest risk in the Indian Himalayas. The classification was carried out based on frequent trigger mechanism of GLOF events and to facilitate even distribution of lakes into very high, high, moderate and low rankings of risk. Classification of hazards puts the lakes with avalanches hitting the lake with a steep moraine (>10°) in very high hazard category as they represent the two most frequent triggering mechanisms. The high hazard category contains the lakes which either have an avalanche hitting the lake or steep moraine with an ice core. The lakes with an ice core have been given a higher hazard ranking than a lake solely with steep moraine, as it may trigger dam settlement or piping. Moderate hazard includes any lake with either an unstable moraine or a rockfall entering the lake. Rockfall was classified in moderate ranking as there have been only three recorded GLOF events triggered by a rockfall (Byers et

al., 2019; Emmer & Cochachin, 2013; Richardson & Reynolds, 2000). Lastly, lakes with low hazard are the ones with gentle (<10°) moraine and no mass entering the lake (Figure 2(b)).

Classification of downstream impacts puts the lake threatening a large number (100) of buildings and at least one hydropower system into very high downstream impact category, the lakes impacting either a large number of buildings or a hydropower system into high downstream impact category and the lakes threatening a small number of buildings or bridges in moderate downstream impact category. The lakes threatening no buildings and bridges were put into low downstream impact category. The criteria for the classification of risk were obtained from Rounce et al., (2017) which is an updated approach from Worni et al., (2013) and Rounce et al., (2016), it states that any combination of very high downstream impact and high hazard or vice versa will lead to the categorisation of the lake in very high-risk category. Subsequently, the lakes with high hazard and high downstream impact were categorised in the high-risk category. Any combination of low hazard and medium downstream impact or vice versa along with low hazard and low downstream impact were categorised in the low-risk category. Lastly, the remaining were categorised in moderate risk category (Figure 2(c)).

3 Results

3.1 Inventory

In the Indian Himalayas, 329 glacial lakes (>0.05 km^2) were inventoried for the year 2018. These lakes were scattered in 4 states (Himachal Pradesh, Uttarakhand, Sikkim and Arunachal Pradesh) and 2 union territories (Ladakh, Jammu and Kashmir) of India. State-wise distribution of these lakes reveals that the union territories encompass 98 (30%) glacial lakes. Himachal Pradesh comprises 36 (11%) glacial lakes, Uttarakhand comprises 22 (7%) glacial lakes, Sikkim comprises 88 (27%) glacial lakes and Arunachal Pradesh comprises 85 (26%) glacial lakes (Figure 3(a)). Major river basin wise distribution reveals that the Indus basin contains 134 (41%) glacial lakes, Ganga basin contains 22 (7%) glacial lakes and Brahmaputra basin contains 173 (52%) glacial lakes (Figure 3(c)). These lakes covered an area of 65.80 ± 4.37 km^2 in 2018. Lake size distribution of these lakes revealed that 129 (39%) lakes were smaller than 0.1 km^2, 178 (54%) had size ranging between 0.1 km^2 to 0.5 km^2 and only 22 (7%) were found to be greater than 0.5 km^2. Distribution of lakes according to their type revealed that moraine-dammed lakes account for 154 (47%) lakes, followed by 57 ice-dammed lakes (17%), 31 bedrock dammed lake (9%) and 87 other lakes such as erosional and debris dammed lakes (26%) (Figure 3(b) and 3(d)). Elevation profile of the lakes revealed that the lakes ranged from 3000 (meters above sea level) m.a.s.l to 5661 m.a.s.l with the mean elevation value of 4484 m.a.s.l. The lakes present above the elevation of 5000 m.a.s.l were predominantly ice-dammed and moraine-dammed. Almost all bedrock dammed lakes were present below 5000 m.a.s.l, whereas other lakes were uniformly distributed among all the elevation zones (Figure 3(e)). It was observed in the Indus and Ganga basins, large-sized lakes were present below 4400 m.a.s.l whereas for Brahmaputra basin all the large-sized lakes were located above the elevation 4900 m.a.s.l (Figure 3(f)). All the lakes of the union territories and Himachal Pradesh were located within the Indus basin, the lakes of Uttarakhand were located within the Ganga basin, whereas all the lakes of Sikkim and Arunachal Pradesh were located within the Brahmaputra basin. In 1993, the area covered by these lakes was 56.8 ± 15.69 km^2 which increased to 65.80 ± 4.37 km^2 by 2018, i.e., a 15.84 % increase in lake area over 25 years. Similar increase in lake area has been observed in Tibetan plateau (Zhang et al., 2014), Nepal (Nie et al., 2013), Bhutan

(Komori, 2008), Tien Shan (Narama et al., 2010), Central Andes (Wilson et al., 2018) and Western Greenland (Carrivick & Quincey, 2014).

3.2 Hazard

The determination of potential hazards was carried out by modelling moraine stability, avalanche, rockfall, GLOF in the upstream portion of the lake and lake expansion. For avalanche and rockfall, a direct hit on the lake was considered to be any trajectory entering the lake with the starting point located within ± 45º of the major axis of the lake. A direct hit may have grave implications on wave run-up and moraine stability. Modelling of dynamic failure revealed that out of 329 lakes, 36 (11%) are susceptible to an avalanche entering the lake, 52 (16%) are susceptible to a rockfall, and 37 (11%) are susceptible to an upstream GLOF. It was also observed that only 8 (22%) out of 36 avalanches and 15 (29%) out of 52 rockfalls were entering the lake with a direct hit which implied that most of the mass entering the lake was along its minor axis. Concerning moraine stability, 247 (75%) lakes have an unstable moraine (average SLA angle > 10º), and 80 (24) have ice cores present in their damming structure. Assessment of lake expansion revealed that from 1993 to 2018, 64 (19.5%) lakes significantly expanded and 6 (2%) lakes significantly drained (Figure 4).

Modelled hazards were used to classify the lakes into various hazard categories, i.e., 28 lakes were categorised as very high hazard, 50 as high hazard, 198 as moderate hazard and 53 as low hazard. Sikkim has the maximum number (20) of very high hazard lakes followed by the union territories of Ladakh and Jammu and Kashmir (4). The state of Himachal Pradesh and Arunachal Pradesh contains two very high hazard lakes each, whereas Uttarakhand has no very high hazard lake. River basin wise, Brahmaputra basin has 20 very high hazard lakes, followed by 6 in Indus basin and 2 in the Ganga basin. Classification of very high hazard lakes, based on type revealed that 20 were moraine dammed, 7 were ice-dammed, and 1 was the other lake. This is attributed due to elevation dependence and direct connection of ice-dammed and moraine-dammed lake with their parent glaciers which make them highly susceptible to avalanches. Elevation dependence of lakes revealed that all the very high hazard lakes were lying above the elevation range of 4000 m (Figure 5(a)). The commonly known very high hazard lakes in the Indian Himalayas include Shakho Cho, Khangchung Tso, Bhale Pokhri Lake and Goecha Lake. Other commonly known high hazard lakes include South Lhonak Lake, Basudhara Tal, Lam Dal Lake, Shaushar Lake, Gadsar Lake, and Lolgul Gali Lake. Few lakes such as Geepang Gath (moderate hazard), Chandra Tal (moderate hazard), Samudri Tapu (moderate hazard) and Gurudongmar (moderate hazard) were not classified as critical because of no avalanche trajectories entering the lake, as well as unavailability of ice cores in damming moraine.

The sensitivity test conducted by varying the "look-up" for avalanche by ± 3º did not alter the number of lakes prone to avalanche. In case of rockfall, the decrease in look-up angle to 17º increased the number of lakes susceptible to rockfall from 52 to 62 and categorised two low hazard lakes to moderate hazard category, whereas increasing the look-up angle to 23º, reduced the number of lakes prone to rockfall from 52 to 35 and changed the hazard ranking of 4 lakes

from moderate to low. Unlike Rounce et al., 2017, the change in look-up angle for rockfall induced a substantial change in lake categorisation.

3.3 Downstream impact

There are 217 lakes that inundated at least 20 buildings while 138 inundated at least 100 buildings; nine lakes were identified to inundate more than 1000 buildings. Six lakes inundating more than 1000 buildings were located in the union territories of Jammu and Kashmir and Ladakh whereas three lakes were located in Uttarakhand (Figure 6(c)). The number of buildings inundated varied from 0 to 2010, with a median number of 54. The number of lakes that inundated at least one hydropower system was 67 whereas the number of lakes that inundated two hydropower systems was 15 (Figure 6(b)). The number of bridges inundated ranged from 0 to 17 with a median value of 4 (Figure 6(a)).

The ranking of downstream impact by considering the 100 buildings threshold to differentiate between large and small number of buildings classified 51 lakes as very high downstream impact, 87 as high downstream impact, 148 as moderate downstream impact and 43 as low downstream impact. The threshold of 100 buildings helped in distributing the lakes uniformly. 51 lakes out of 67 that inundated at least one hydropower system also inundated 100 buildings. This shows that hydropower systems are located near the areas of settlements. Altering the building threshold to 50 buildings increased the number of lakes in very high downstream impact category by 3 and high downstream category by 30. Union territories of Jammu and Kashmir and Ladakh consist of the highest number of very high downstream impact lakes, followed by Sikkim, Uttarakhand, Himachal Pradesh and lastly Arunachal Pradesh, which has no lake that shows very high downstream impact. Most of the lakes with very high downstream impact were located below the elevation of 5000 m except for 3 lakes in Uttarakhand and 1 lake in Sikkim (Figure 5(b)). Some of the commonly known lakes with very high downstream impact are Sheshnag Lake, Tsomgo Lake and Hangu Lake.

The uncertainty associated with PFV estimation in case where the computation was based on SLA analysis of lake was found to be ±44%, whereas, in the case of avalanche and rockfall, the uncertainty values were found to be ±68% and ±52% respectively. It was observed that these uncertainty values were majorly caused due to error in-depth estimation (Importance = 98%, 95%, 91% in case of SLA, avalanche and rockfall, respectively) rather than the error in area estimation.

3.4 Risk

The risk categorisation of glacial lakes was based on the criteria described in Figure 2(c). A total of 23 lakes were classified as very high risk, 50 were classified as high risk, 195 were classified as moderate risk, and 61 were classified as low risk. Out of 51 lakes that were characterised as very high downstream impact, merely 10 were categorised as very high risk due to their moderate hazard. State-wise distribution of very high-risk lakes revealed that the union territories of Ladakh and Jammu and Kashmir have 4 very high-risk lakes, Uttarakhand has 2 very high-risk lakes and Sikkim has 17 very high-risk lakes, whereas Himachal Pradesh and Arunachal Pradesh have no very high-risk lakes (Figure 7). There was no apparent trend between risk and elevation of lakes (Figure 5(c)). Table 1 shows the lake details, associated hazard, downstream impact, and potential risk of the lakes recognised as very high-risk lakes and their confrontation against other studies in the Indian Himalayas (Abdul Hakeem et al., 2018; Aggarwal et al., 2017; Ives et al., 2010; Raj & Kumar, 2016; Worni et al., 2013).

4 Discussions

4.1 Glacial lake inventory

This study identified 329 glacial lakes in the Indian Himalayas, which strongly agrees with previous studies (Aggarwal et al., 2017; Fujita et al., 2013; Ives et al., 2010; Worni et al., 2013; Zhang et al., 2015) (Supplementary table sheet 3, 4, 5, 6 and 7). The threshold of lakes above the elevation of 3000 meters to select the glacial lakes was applied instead of the threshold used by previous studies (only moraine-dammed lakes for Fujita et al., 2013 and any lakes within 10 km of glacier boundaries for Worni et al., 2013), as the uncertainty associated with debris-covered glaciers in these inventories may range up to 30% and it can significantly alter the study area (Yao et al., 2012) and use of only moraine-dammed lakes may lead to underestimation of potential GLOF hazard.

The lakes that did not show any significant expansion between 1993 and 2018 were compared for the year 2018 against the lake area measurement by Fujita et al., (2013). As Fujita et al., (2013) only considered moraine-dammed lakes, the comparison was made only for 128 lakes that were common for both the studies. The mean difference in lake area between these studies was found to be 0.0183 km^2 which is comparable with the assumption of error linked with lake delineation which ranged from 0.0127 to 0.1337 km^2 with mean value of 0.0296 km^2. Therefore, the assumption used to measure lake error, i.e., perimeter multiplied by half the pixel size is reasonable.

The maximum distance of lake from glaciers experiencing an avalanche and rockfall are 607.5 and 5079.9 m respectively; therefore, for the studies focusing on dynamic failures, the distance threshold of 10 km can be reasonably adopted. Lake distance of steep moraine lakes revealed that there are 42 lakes with steep moraine that are located beyond 10 km of glacier boundaries, therefore, for studies incorporating self-destructive failure, the distance threshold of 10 km may lead to under-representation of glacial lakes.

4.2 Hazard and downstream impact

This study modelled the most frequent triggers of GLOF such as avalanche or rockfall hit, Upstream GLOF, stability of the damming moraine and presence of ice cores. Other triggers of GLOF include extreme climatic events and seismic activities. These triggers were integrally assessed by the studied hazard parameters as an extreme climatic event, or seismic activity will ultimately alter the hydrostatic pressure on the damming moraine which will more likely trigger the failure of an unstable moraine in comparison to a stable one. The impact of remediation measures was not studied as there has been only one such effort at South Lhonak Lake, Sikkim. The lowering of the lake was by 3 m, i.e., well within the associated error of the DEM (RMSE = 17 m), therefore it was not possible to make any noticeable inferences for its impact on the hazard.

The major struggle accompanied with any hazard assessment is the technique to represent the parameters in terms of its hazard category. This is especially perplexing, as these events are unpredictable and usually occur in a remote location. Therefore, the data from past events and the knowledge of their triggers are limited. Another difficulty associated with hazard assessment is that these events are interconnected, i.e., one trigger can evolve into another. Falátková, (2016) addresses this issue by demonstrating that the destabilisation and breach of damming moraine may take place by the coupled effect of an avalanche, melting of ice cores, increase in hydrostatic pressure and the effect over time. Additionally, Emmer & Cochachin,

(2013) described the combined effect of ice cores, hydrostatic pressure and time in a single hazard parameter called as self-destruction. The SLA analysis illustrated by Fujita et al., (2013) inherently takes into account the combined impact of various triggers as it focusses on the failure of the moraine irrespective of their triggering mechanism.

These aspects of hazard analysis imply that while the underlying triggering mechanisms are understood for GLOF, there is still significant uncertainty concerning how the interconnection of these triggers affects the hazard. These inherent uncertainties prevent the quantitative hazard assessment by assignment of weights to various hazard parameters, eg., in the case of Bolch et al., (2011) and Wang et al., (2013). To overcome this, a framework was adopted to reflect the most hazardous situations by frequency of the various triggering mechanisms involved. The expansion of glacial lakes was not used as a parameter of GLOF assessment as Rounce et al., (2017) applied the expansion model to predict the further expansion of glacial lakes in Nepal Himalayas and observed that 15 out of 22 glacial lakes with significant expansion were incapable of further growth and only 1 lake out of 136 exhibited a change in its hazard assessment.

For downstream impact assessment, the GLOF extents were conservatively assessed using the stochastic MC-LCP model by quantifying potential buildings, hydropower systems, and bridges located within the inundation regions. Large scale applicability, inexpensive computations, and consideration of DEM uncertainty are the benefits of MC-LCP model whereas no accountability for any variations in PFVs is the limitation. It should be noted that GLOFs at Lmja Tso and Dig Tsho had PFV of 33.5×10^6 m^3 (Somos-Valenzuela et al., 2016) and 5×10^6 m^3 (Vuichard & Zimmermann, 1987), respectively. Consequently, MC-LCP is producing flood extent linked with large PFV values. A good example describing this is by Khangchung Tso and Lake 228. Both of these lakes have similar flood extent despite having very different PFV of 19.928×10^6 m^3 and 0.7612×10^6 m^3. Figure 8 describes the distribution of lakes at different PFV ranges. It shows that the number of lakes dramatically reduces beyond 5×10^6 m^3. The figure also shows that most of the lakes with PFV higher than 5×10^6 m^3 are located in Arunachal Pradesh and Sikkim. Past GLOF events of Dig Tsho and Tam Pokhri shows that PFV of 5×10^6 m^3 is significant enough to produce high socio-economic damage to downstream communities. Conversely, a lake outburst near Chorabari glacier in Uttarakhand with PFV of just 0.43×10^6 m^3 caused catastrophic damage and killed more than 4000 people in 2013. Therefore, the risk assessment should be based on downstream impact rather than PFV. We assumed the runout distance for each lake to be 50 km, beyond which the waves were considered to be relatively small in comparison to structures located outside the main channel. This assumption is consistent with most of the past events (Rafiq et al., 2019; Vuichard & Zimmermann, 1987) Whereas, due to exceptions such as Luggye Tsho (Reynolds, 2014; Richardson & Reynolds, 2000) where the runout length of 200 km was observed, determination of runout length should be based on the application of physically based hydrodynamic model using variable discharge values, this can also be incorporated in MC-LCP model by the use of cost function based on runout distance. Additionally, due to the presence of artefacts in the DEM, the river network obtained did not coincide with the actual river path for few lakes (Lake 284, Lake 285, Lake 286, etc), for such lakes the river network obtained using reconditioned DEM with 20 m vertical buffer was considered as flood extent instead of MC-LCP output. Improved locations of hydropower systems and updated inventory of buildings can significantly improve the downstream impact assessment. Nevertheless, this study can provide

a conservative estimate of flood extents for each lake that can provide vital information for planning risk mitigation measures.

4.3 Risk

This study is meant to assist stakeholders in identifying critical glacial lake that needs an additional field survey. With the available financial resources, field investigation and hydrodynamic modelling of each of these lakes are impractical, but field-based assessment on a few of these lakes to validate remotely sensed based assessment can be useful. The framework for this study has been designed in a manner that data from hazard and downstream impact assessment can even be used by decision-makers who may have an alternate way on the classification of these glacial lakes. This study sought to balances both social and economic effects; Conversely, if economic impacts were to be prioritized, then the lakes affecting more hydropower systems should have been given higher downstream impact, e.g., Bhale Pokhri Lake, Goecha La Lake, Hangu Lake, and Tsomgo Lake, etc. Alternatively, if the social impact were to be prioritized, the lakes affecting more number of buildings should have been given the highest downstream impact, e.g., Lake 12, 56, etc.

The classification showed here were established by prioritizing the lakes based on their hazard and downstream impact, while on the contrary, a common way to priorities the lake impact is based on higher PFV. Hazard, downstream impact and risk of lakes having PFV higher than 5×10^6 m^3 (PFV of Dig Tsho) are illustrated in Table 2; there are total 32 lakes in Indian Himalayas that have PFV exceeding 5×10^6 m^3 among which 7 are at very high risk, 3 are at high risk and 22 lakes are at moderate risk. Gurudongmar Lake has the largest PFV due to its large size (1.120 km^2) and steep moraine (42.47º). Shakho Cho Lake being one of the most dangerous lake in the Indian Himalayas is equipped with water level gauging instrument to monitor high rise in lake. Despite being a well-studied (Worni et al., 2013, 2014) lake in Indian Himalayas, no mitigation measures have been taken so far, and the lake appears to be at very high risk due to the potential of avalanche and rockfall. Other notable lakes that were not included in the list but are at very high risk are Lake 153, Lake 164 and Lake 218. Physically-based hydrodynamic modelling of GLOF from these lakes would significantly improve the hazard and downstream risk assessment and aid the stakeholders in taking decisions related to risk mitigation measures.

4.4 Implications for stakeholders

Accurate identification of potentially dangerous glacial lake is challenging, but yet a crucial task and is vital to maintain the trustworthiness of the decision-makers and local communities. Generally, the regional studies assess different parameters to identify potential hazard associated with glacial lakes, and therefore the obtained results depict very different results. Therefore, we recommend the stakeholders to base the decision criteria on the analysis based on new and more comprehensive data, more sophisticated analysis, enhanced understanding of system, and robust model simulations with wider consideration of uncertainties. The important characteristics to prioritise the glacial lake studies should be (1) credibility of the evidence that the applied model relies upon; (2) standardized application of methodology; (3) inclusion of most frequent GLOF triggers; and (4) the level of details in the estimated probable impact.

The primary objective of policy-research linkage should be to convey advanced scientific data and technology to planning, mitigation and ultimately, reduce the projected risk. One crucial aspect of these hazard assessments is the consideration of worst-case scenarios, something that is not very likely and this must be appropriately communicated to the decision-makers.

Secondly, there should be formal communication channels between policy-makers and research scientists to enable precise knowledge transfer and lastly, although the associated risk with the glacial hazards are very high, yet are mostly indeterminate, and the present tendency of grossly overstating the results in terms of both hazard and potential catastrophe needs to be realized and strictly discouraged.

5 Conclusions

The present study implemented a comprehensive evaluation of hazard, downstream impact and associated risk for 329 glacial lakes with size greater than 0.05 km^2 in the Indian Himalayas. The implemented methodology assesses the most frequent triggers based on the detailed literature review which includes avalanche, rockfall, stability of the damming moraine, expansion rate, and presence of ice cores. The results indicated that glacial lakes expanded by 15.84% between 1993 and 2018, where 64 lakes significantly expanded and 6 lakes significantly drained; 36 lakes are susceptible to an avalanche where most of the hit is expected along the minor axis. Application of stochastic flood model reveals that 67 glacial lakes contain at least one hydropower system along their flow path. The risk assessment indicates that there are 23 very high-risk lakes and 50 high-risk lakes in the Indian Himalayas. The main objective of the study was to implement an objective methodology that was least subjective as possible. Conversely, with the present state of knowledge regarding triggering mechanisms of GLOF and available remotely sensed satellite data, there is a certain level of subjectiveness that is inherently inescapable in these first pass GLOF assessments.

We recommend the use of downstream impact along with potential flood volume for both dynamic and self-destructive failures to rank glacial lakes as with sizeable flood volume, proximities of the area of settlement and socio-economic consequence are equally essential to recognise a lake as potentially dangerous. Some of the notable lakes with very high PFV include Gurudongmar Lake, Tso Lhamo Lake and J R B Lake; whereas, some of the lakes with high PFV and very high risk include Khangchung Tso and Shakho Cho. The use of hydrodynamic model, along with field-based assessments is strongly suggested before implementing any risk mitigation measures. Additionally, as higher temporal resolution DEMs become available the hazard assessment should be repeated as it will enable DEM differencing which will significantly improve the identification of ice cores and the modelling of dynamic failures.

Acknowledgements

This work was financially supported by the Ministry of Environment, Forest and Climate Change, Government of India by research project (GBPNI/NMHS-2017-18/SG10) under the National Mission on Himalayas Studies (NMHS) Program. The authors would also like to thank David R. Rounce for his encouragement and support to this study, and Ashim Sattar for

the modelled flood extent of South Lhonak Lake, Sikkim. The dataset used in the study can be accessed online from

https://earthexplorer.usgs.gov/

https://lpdaac.usgs.gov/

https://www.glims.org/RGI/rgi50_files/rgi50.zip

http://www.indiaenvironmentportal.org.in/files/file/Hydro-power.pdf

https://www.openstreetmap.org

References

Abdul Hakeem, K., Abirami, S., Rao, V. V, Diwakar, P. G., & Dadhwal, V. K. (2018). Updated Inventory of Glacial Lakes in Teesta Basin Using Remote Sensing Data for Use in GLOF Risk Assessment. *Journal of the Indian Society of Remote Sensing*, *46*(3), 463–470. https://doi.org/10.1007/s12524-017-0699-1

Aggarwal, S., Rai, S. C., Thakur, P. K., & Emmer, A. (2017). Inventory and recently increasing GLOF susceptibility of glacial lakes in Sikkim, Eastern Himalaya. *Geomorphology*, *295*, 39–54. https://doi.org/10.1016/j.geomorph.2017.06.014

Alean, J. (1985). Ice Avalanches: Some Empirical Information about their Formation and Reach. *Journal of Glaciology*, *31*(109), 324–333. https://doi.org/10.3189/S0022143000006663

Allen, S. K., Rastner, P., Arora, M., Huggel, C., & Stoffel, M. (2016). Lake outburst and debris flow disaster at Kedarnath, June 2013: hydrometeorological triggering and topographic predisposition. *Landslides*, *13*(6), 1479–1491. https://doi.org/10.1007/s10346-015-0584-3

Arendt, A., Bliss, A., Bolch, T., Cogley, J. G., Gardner, A. S., Hagen, J. O., et al. (2015). Randolph Glacier Inventory–A dataset of global glacier outlines: Version 5.0. *Global Land Ice Measurements from Space, Boulder Colorado, USA*.

Bajracharya, S. R., & Mool, P. (2009). Glaciers, glacial lakes and glacial lake outburst floods in the Mount Everest region, Nepal. *Annals of Glaciology*, *50*(53), 81–86. https://doi.org/10.3189/172756410790595895

Bolch, T., Peters, J., Yegorov, A., Pradhan, B., Buchroithner, M., & Blagoveshchensky, V. (2011). Identification of potentially dangerous glacial lakes in the northern Tien Shan. *Natural Hazards*, *59*(3), 1691–1714. https://doi.org/10.1007/s11069-011-9860-2

Buchroithner, M. F., Jentsch, G., & Wanivenhaus, B. (1982). Monitoring of recent geological events in the Khumbu area (Himalaya, Nepal) by digital processing of landsat MSS data. *Rock Mechanics*, *15*(4), 181–197. https://doi.org/10.1007/BF01240589

Byers, A. C., Rounce, D. R., Shugar, D. H., Lala, J. M., Byers, E. A., & Regmi, D. (2019). A rockfall-induced glacial lake outburst flood, Upper Barun Valley, Nepal. *Landslides*, *16*(3), 533–549. https://doi.org/10.1007/s10346-018-1079-9

Carrivick, J. L., & Quincey, D. J. (2014). Progressive increase in number and volume of ice-marginal lakes on the western margin of the Greenland Ice Sheet. *Global and Planetary Change*, *116*, 156–163. https://doi.org/10.1016/j.gloplacha.2014.02.009

Carrivick, J. L., & Rushmer, E. L. (2006). Understanding high-magnitude outburst floods. *Geology Today*, *22*(2), 60–65. https://doi.org/10.1111/j.1365-2451.2006.00554.x

Carrivick, J. L., & Tweed, F. S. (2013). Proglacial lakes: character, behaviour and geological importance. *Quaternary Science Reviews*, *78*, 34–52. https://doi.org/10.1016/j.quascirev.2013.07.028

Carrivick, J. L., & Tweed, F. S. (2016). A global assessment of the societal impacts of glacier outburst floods. *Global and Planetary Change*, *144*, 1–16. https://doi.org/10.1016/j.gloplacha.2016.07.001

Chen, X., Cui, P., Li, Y., Yang, Z., & Qi, Y. (2007). Changes in glacial lakes and glaciers of post-1986 in the Poiqu River basin, Nyalam, Xizang (Tibet). *Geomorphology*, *88*(3–4), 298–311. https://doi.org/10.1016/j.geomorph.2006.11.012

Chen, Y., Xu, C., Chen, Y., Li, W., & Liu, J. (2010). Response of glacial-lake outburst floods to climate change in the Yarkant River basin on northern slope of Karakoram Mountains, China. *Quaternary International*, *226*(1–2), 75–81. https://doi.org/10.1016/j.quaint.2010.01.003

Cogley, J. G. (2016). Glacier shrinkage across High Mountain Asia. *Annals of Glaciology*, *57*(71), 41–49. https://doi.org/10.3189/2016AoG71A040

Collins, B. D., & Jibson, R. W. (2015). *Assessment of existing and potential landslide hazards resulting from the April 25, 2015 Gorkha, Nepal earthquake sequence*. US Geological Survey. https://doi.org/https://doi.org/10.3133/ofr20151142

Cook, S. J., & Quincey, D. J. (2015). Estimating the volume of Alpine glacial lakes. *Earth Surface Dynamics Discussions*, *3*(3), 909–940. https://doi.org/10.5194/esurfd-3-909-2015

Cui, P., Dang, C., Cheng, Z., & Scott, K. M. (2011). Debris Flows Resulting From Glacial-Lake Outburst Floods in Tibet, China. *Physical Geography*, *31*(6), 508–527. https://doi.org/10.2747/0272-3646.31.6.508

Drusch, M., Del Bello, U., Carlier, S., Colin, O., Fernandez, V., Gascon, F., et al. (2012). Sentinel-2: ESA's Optical High-Resolution Mission for GMES Operational Services. *Remote Sensing of Environment*, *120*, 25–36. https://doi.org/10.1016/j.rse.2011.11.026

Emmer, A, Vilímek, V., Huggel, C., Klimeš, J., & Schaub, Y. (2016). Limits and challenges to compiling and developing a database of glacial lake outburst floods. *Landslides*, *13*(6), 1579–1584. https://doi.org/10.1007/s10346-016-0686-6

Emmer, Adam. (2018). GLOFs in the WOS: bibliometrics, geographies and global trends of research on glacial lake outburst floods (Web of Science, 1979–2016). *Natural Hazards and Earth System Sciences*, *18*(3), 813–827. https://doi.org/10.5194/nhess-18-813-2018

Emmer, Adam, & Cochachin, A. (2013). The causes and mechanisms of moraine-dammed lake failures in the Cordillera Blanca, North American Cordillera, and Himalayas. *AUC Geographica*, *48*(2), 5–15.

Falátková, K. (2016). Temporal analysis of GLOFs in high-mountain regions of Asia and

assessment of their causes. *AUC Geographica*, *51*(2), 145–154.

Fujita, K., Sakai, A., Takenaka, S., Nuimura, T., Surazakov, A. B., Sawagaki, T., & Yamanokuchi, T. (2013). Potential flood volume of Himalayan glacial lakes. *Natural Hazards and Earth System Sciences*, *13*(7), 1827–1839. https://doi.org/10.5194/nhess-13-1827-2013

Gardelle, J., Arnaud, Y., & Berthier, E. (2011). Contrasted evolution of glacial lakes along the Hindu Kush Himalaya mountain range between 1990 and 2009. *Global and Planetary Change*, *75*(1–2), 47–55. https://doi.org/10.1016/j.gloplacha.2010.10.003

Huggel, C., Haeberli, W., Kääb, A., Bieri, D., & Richardson, S. (2004). An assessment procedure for glacial hazards in the Swiss Alps. *Canadian Geotechnical Journal*, *41*(6), 1068–1083. https://doi.org/10.1139/t04-053

Ives, J. D., Shrestha, R. B., & Mool, P. K. (2010). *Formation of glacial lakes in the Hindu Kush-Himalayas and GLOF risk assessment*. ICIMOD Kathmandu.

Kääb, A., Berthier, E., Nuth, C., Gardelle, J., & Arnaud, Y. (2012). Contrasting patterns of early twenty-first-century glacier mass change in the Himalayas. *Nature*, *488*(7412), 495–498. https://doi.org/10.1038/nature11324

Kanti, T., Flemming, G., Madhu, J., & Kuldeep, J. (2019). Extreme rainfall and vulnerability assessment : case study of Uttarakhand rivers. *Natural Hazards*, (0123456789). https://doi.org/10.1007/s11069-019-03765-3

King, O., Quincey, D. J., Carrivick, J. L., & Rowan, A. V. (2017). Spatial variability in mass loss of glaciers in the Everest region, central Himalayas, between 2000 and 2015. *The Cryosphere*, *11*(1), 407–426. https://doi.org/10.5194/tc-11-407-2017

King, O., Dehecq, A., Quincey, D., & Carrivick, J. (2018). Contrasting geometric and dynamic evolution of lake and land-terminating glaciers in the central Himalaya. *Global and Planetary Change*, *167*, 46–60. https://doi.org/10.1016/j.gloplacha.2018.05.006

Komori, J. (2008). Recent expansions of glacial lakes in the Bhutan Himalayas. *Quaternary International*, *184*(1), 177–186. https://doi.org/10.1016/j.quaint.2007.09.012

Linsbauer, A., Frey, H., Haeberli, W., Machguth, H., Azam, M. F., & Allen, S. (2016). Modelling glacier-bed overdeepenings and possible future lakes for the glaciers in the Himalaya—Karakoram region. *Annals of Glaciology*, *57*(71), 119–130.

Liu, J., Tang, C., & Cheng, Z. (2013). The two main mechanisms of glacier lake outburst flood in Tibet, China. *Journal of Mountain Science*, *10*(2), 239–248.

Maharjan, S. B., Mool, P. K., Lizong, W., Xiao, G., Shrestha, F., Shrestha, R. B., et al. (2018). *The status of glacial lakes in the Hindu Kush Himalaya-ICIMOD Research Report 2018/1 (2018). ICIMOD Research Report*. International Centre for Integrated Mountain Development (ICIMOD).

Maurer, J. M., Schaefer, J. M., Rupper, S., & Corley, A. (2019). Acceleration of ice loss across the Himalayas over the past 40 years. *Science Advances*, *5*(6), eaav7266. https://doi.org/10.1126/sciadv.aav7266

McFEETERS, S. K. (1996). The use of the Normalized Difference Water Index (NDWI) in the delineation of open water features. *International Journal of Remote Sensing*, *17*(7), 1425–1432. https://doi.org/10.1080/01431169608948714

Mool, P. K., Maskey, P. R., Koirala, A., Joshi, S. P., Wu, L., Shrestha, A. B., et al. (2011). Glacial Lakes and Glacial Lake Outburst Floods in Nepal. *Icimod*, 1–109. https://doi.org/978 92 9115 193 6

Nagai, H., Ukita, J., Narama, C., Fujita, K., Sakai, A., Tadono, T., et al. (2017). Evaluating the Scale and Potential of GLOF in the Bhutan Himalayas Using a Satellite-Based Integral Glacier–Glacial Lake Inventory. *Geosciences*, *7*(3), 77. https://doi.org/10.3390/geosciences7030077

Narama, C., Kääb, A., Duishonakunov, M., & Abdrakhmatov, K. (2010). Spatial variability of recent glacier area changes in the Tien Shan Mountains, Central Asia, using Corona (~1970), Landsat (~2000), and ALOS (~2007) satellite data. *Global and Planetary Change*, *71*(1–2), 42–54. https://doi.org/10.1016/j.gloplacha.2009.08.002

Nie, Y., Liu, Q., & Liu, S. (2013). Glacial lake expansion in the Central Himalayas by Landsat images, 1990–2010. *PLoS One*, *8*(12), e83973.

Nie, Y., Liu, Q., Wang, J., Zhang, Y., Sheng, Y., & Liu, S. (2018). An inventory of historical glacial lake outburst floods in the Himalayas based on remote sensing observations and geomorphological analysis. *Geomorphology*, *308*, 91–106. https://doi.org/10.1016/j.geomorph.2018.02.002

Nuimura, T., Sakai, A., Taniguchi, K., Nagai, H., Lamsal, D., Tsutaki, S., et al. (2014). The GAMDAM Glacier Inventory: a quality controlled inventory of Asian glaciers. *The Cryosphere Discussions*, *8*(3), 2799–2829. https://doi.org/10.5194/tcd-8-2799-2014

Osti, R., & Egashira, S. (2009). Hydrodynamic characteristics of the Tam Pokhari glacial lake outburst flood in the Mt. Everest region, Nepal. *Hydrological Processes*, *23*(20), 2943–2955. https://doi.org/10.1002/hyp.7405

Osti, R., Bhattarai, T. N., & Miyake, K. (2011). Causes of catastrophic failure of Tam Pokhari moraine dam in the Mt. Everest region. *Natural Hazards*, *58*(3), 1209–1223. https://doi.org/10.1007/s11069-011-9723-x

Rafiq, M., Romshoo, S. A., Mishra, A. K., & Jalal, F. (2019). Modelling Chorabari Lake outburst flood, Kedarnath, India. *Journal of Mountain Science*, *16*(1), 64–76. https://doi.org/10.1007/s11629-018-4972-8

Raj, K. B. G., & Kumar, K. V. (2016). Inventory of Glacial Lakes and its Evolution in Uttarakhand Himalaya Using Time Series Satellite Data. *Journal of the Indian Society of Remote Sensing*, *44*(6), 959–976. https://doi.org/10.1007/s12524-016-0560-y

Raj, K. B. G., Remya, S. N., & Kumar, K. V. (2013). Remote sensing-based hazard assessment of glacial lakes in Sikkim Himalaya. *Current Science*, 359–364.

Reynolds, J. M. (2014). Assessing glacial hazards for hydro development in the Himalayas, Hindu Kush and Karakoram. *Water and Energy International*, *71*(3).

Richardson, S. D., & Reynolds, J. M. (2000). An overview of glacial hazards in the Himalayas. *Quaternary International*, *65–66*, 31–47. https://doi.org/10.1016/S1040-6182(99)00035-X

Rounce, D. R., McKinney, D. C., Lala, J. M., Byers, A. C., & Watson, C. S. (2016). A new remote hazard and risk assessment framework for glacial lakes in the Nepal Himalaya. *Hydrology and Earth System Sciences*, *20*(9), 3455–3475. https://doi.org/10.5194/hess-20-3455-2016

Rounce, D. R., Watson, C. S., & McKinney, D. C. (2017). Identification of hazard and risk for glacial lakes in the Nepal Himalaya using satellite imagery from 2000-2015. *Remote Sensing*, *9*(7). https://doi.org/10.3390/rs9070654

Sakai, A., & Fujita, K. (2017). Contrasting glacier responses to recent climate change in high-mountain Asia. *Scientific Reports*, *7*(1), 13717. https://doi.org/10.1038/s41598-017-14256-5

Sattar, A., Goswami, A., & Kulkarni, A. V. (2019). Hydrodynamic moraine-breach modeling and outburst flood routing-A hazard assessment of the South Lhonak lake, Sikkim. *Science of the Total Environment*, *668*, 362–378.

Schwanghart, W., Worni, R., Huggel, C., Stoffel, M., & Korup, O. (2016). Uncertainty in the Himalayan energy–water nexus: estimating regional exposure to glacial lake outburst floods. *Environmental Research Letters*, *11*(7), 074005. https://doi.org/10.1088/1748-9326/11/7/074005

Shukla, A., Garg, P. K., & Srivastava, S. (2018). Evolution of Glacial and High-Altitude Lakes in the Sikkim, Eastern Himalaya Over the Past Four Decades (1975–2017). *Frontiers in Environmental Science*, *6*, 81. https://doi.org/10.3389/fenvs.2018.00081

Somos-Valenzuela, M. A., McKinney, D. C., Byers, A. C., Rounce, D. R., Portocarrero, C., & Lamsal, D. (2015). Assessing downstream flood impacts due to a potential GLOF from Imja Tsho in Nepal. *Hydrology and Earth System Sciences*, *19*(3), 1401–1412. https://doi.org/10.5194/hess-19-1401-2015

Somos-Valenzuela, Marcelo A, Chisolm, R. E., Rivas, D. S., Portocarrero, C., & McKinney, D. C. (2016). Modeling a glacial lake outburst flood process chain: the case of Lake Palcacocha and Huaraz, Peru. *Hydrology and Earth System Sciences*, *20*(6), 2519–2543. https://doi.org/10.5194/hess-20-2519-2016

Tachikawa, T., Hato, M., Kaku, M., & Iwasaki, A. (2011). Characteristics of ASTER GDEM version 2. In *2011 IEEE International Geoscience and Remote Sensing Symposium* (pp. 3657–3660). IEEE. https://doi.org/10.1109/IGARSS.2011.6050017

Ukita, J., Narama, C., Tadono, T., Yamanokuchi, T., Tomiyama, N., Kawamoto, S., et al. (2011). Glacial lake inventory of Bhutan using ALOS data: methods and preliminary results. *Annals of Glaciology*, *52*(58), 65–71. https://doi.org/10.3189/172756411797252293

Veh, G., Korup, O., Roessner, S., & Walz, A. (2018). Detecting Himalayan glacial lake outburst floods from Landsat time series. *Remote Sensing of Environment*, *207*, 84–97. https://doi.org/10.1016/j.rse.2017.12.025

Veh, G., Korup, O., von Specht, S., Roessner, S., & Walz, A. (2019). Unchanged frequency of moraine-dammed glacial lake outburst floods in the Himalaya. *Nature Climate Change*, *9*(5), 379–383. https://doi.org/10.1038/s41558-019-0437-5

Vuichard, D., & Zimmermann, M. (1987). The 1985 Catastrophic Drainage of a Moraine-Dammed Lake, Khumbu Himal, Nepal: Cause and Consequences. *Mountain Research and Development*, *7*(2), 91. https://doi.org/10.2307/3673305

Wang, W., Yao, T., Gao, Y., Yang, X., & Kattel, D. B. (2011). A First-order Method to Identify Potentially Dangerous Glacial Lakes in a Region of the Southeastern Tibetan Plateau. *Mountain Research and Development*, *31*(2), 122.

https://doi.org/10.1659/MRD-JOURNAL-D-10-00059.1

Wang, X., Ding, Y., Liu, S., Jiang, L., Wu, K., Jiang, Z., & Guo, W. (2013). Changes of glacial lakes and implications in Tian Shan, central Asia, based on remote sensing data from 1990 to 2010. *Environmental Research Letters*, *8*(4), 044052. https://doi.org/10.1088/1748-9326/8/4/044052

Watson, C Scott, King, O., Miles, E. S., & Quincey, D. J. (2018). Optimising NDWI supraglacial pond classification on Himalayan debris-covered glaciers. *Remote Sensing of Environment*, *217*, 414–425. https://doi.org/10.1016/j.rse.2018.08.020

Watson, Cameron S, Carrivick, J., & Quincey, D. (2015). An improved method to represent DEM uncertainty in glacial lake outburst flood propagation using stochastic simulations. *Journal of Hydrology*, *529*, 1373–1389. https://doi.org/10.1016/j.jhydrol.2015.08.046

Wilson, R., Glasser, N. F., Reynolds, J. M., Harrison, S., Anacona, P. I., Schaefer, M., & Shannon, S. (2018). Glacial lakes of the Central and Patagonian Andes. *Global and Planetary Change*, *162*, 275–291. https://doi.org/10.1016/j.gloplacha.2018.01.004

Wilson, R., Harrison, S., Reynolds, J., Hubbard, A., Glasser, N. F., Wündrich, O., et al. (2019). The 2015 Chileno Valley glacial lake outburst flood, Patagonia. *Geomorphology*, *332*, 51–65. https://doi.org/10.1016/j.geomorph.2019.01.015

Worni, R., Huggel, C., & Stoffel, M. (2013). Glacial lakes in the Indian Himalayas — From an area-wide glacial lake inventory to on-site and modeling based risk assessment of critical glacial lakes. *Science of The Total Environment*, *468–469*, S71–S84. https://doi.org/10.1016/j.scitotenv.2012.11.043

Worni, R., Huggel, C., Clague, J. J., Schaub, Y., & Stoffel, M. (2014). Coupling glacial lake impact, dam breach, and flood processes: A modeling perspective. *Geomorphology*, *224*, 161–176. https://doi.org/10.1016/j.geomorph.2014.06.031

Yao, T., Thompson, L., Yang, W., Yu, W., Gao, Y., Guo, X., et al. (2012). Different glacier status with atmospheric circulations in Tibetan Plateau and surroundings. *Nature Climate Change*, *2*(9), 663–667. https://doi.org/10.1038/nclimate1580

Zhang, G., Yao, T., Xie, H., Qin, J., Ye, Q., Dai, Y., & Guo, R. (2014). Estimating surface temperature changes of lakes in the Tibetan Plateau using MODIS LST data. *Journal of Geophysical Research: Atmospheres*, *119*(14), 8552–8567.

Zhang, G., Yao, T., Xie, H., Wang, W., & Yang, W. (2015). An inventory of glacial lakes in the Third Pole region and their changes in response to global warming. *Global and Planetary Change*, *131*, 148–157. https://doi.org/10.1016/j.gloplacha.2015.05.013

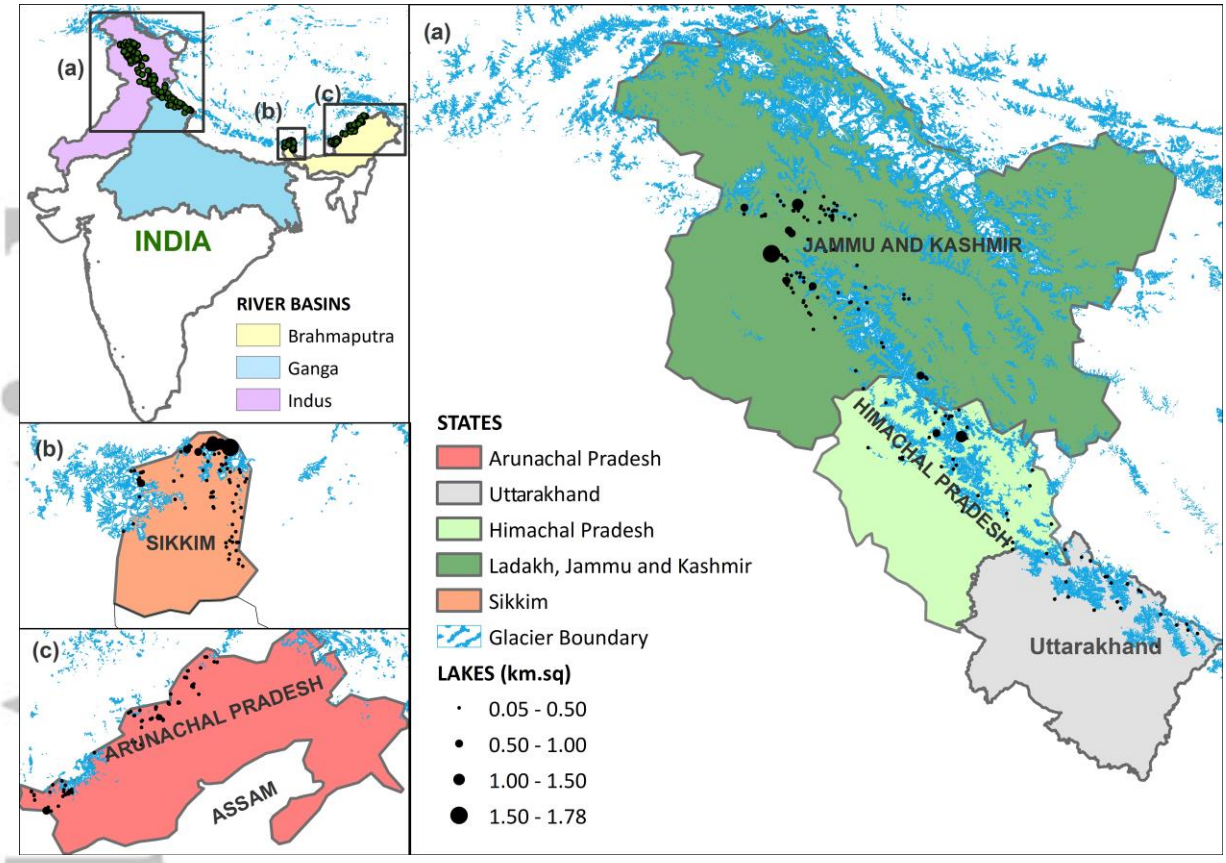

Figure 1. Glacial lakes in Indian Himalayas, along with major river basins and states. Jammu Kashmir shown in the figure has been recently divided into 2 union territories (Jammu and Kashmir, and Ladakh).

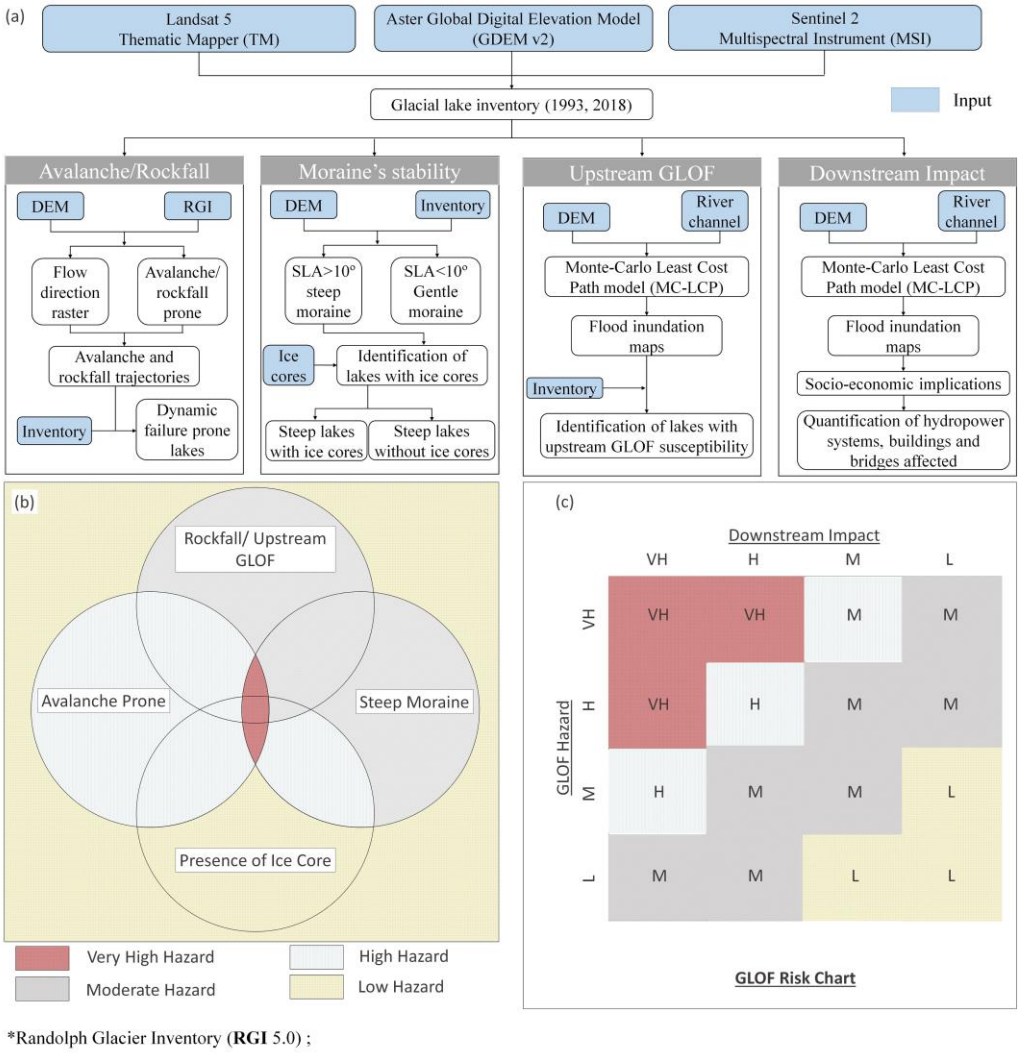

Figure 2. (a) Workflow of method; (b) Hazard classification flow chart represented using Venn diagrams; (c) Risk chart represented as a function of downstream impact and GLOF hazard.

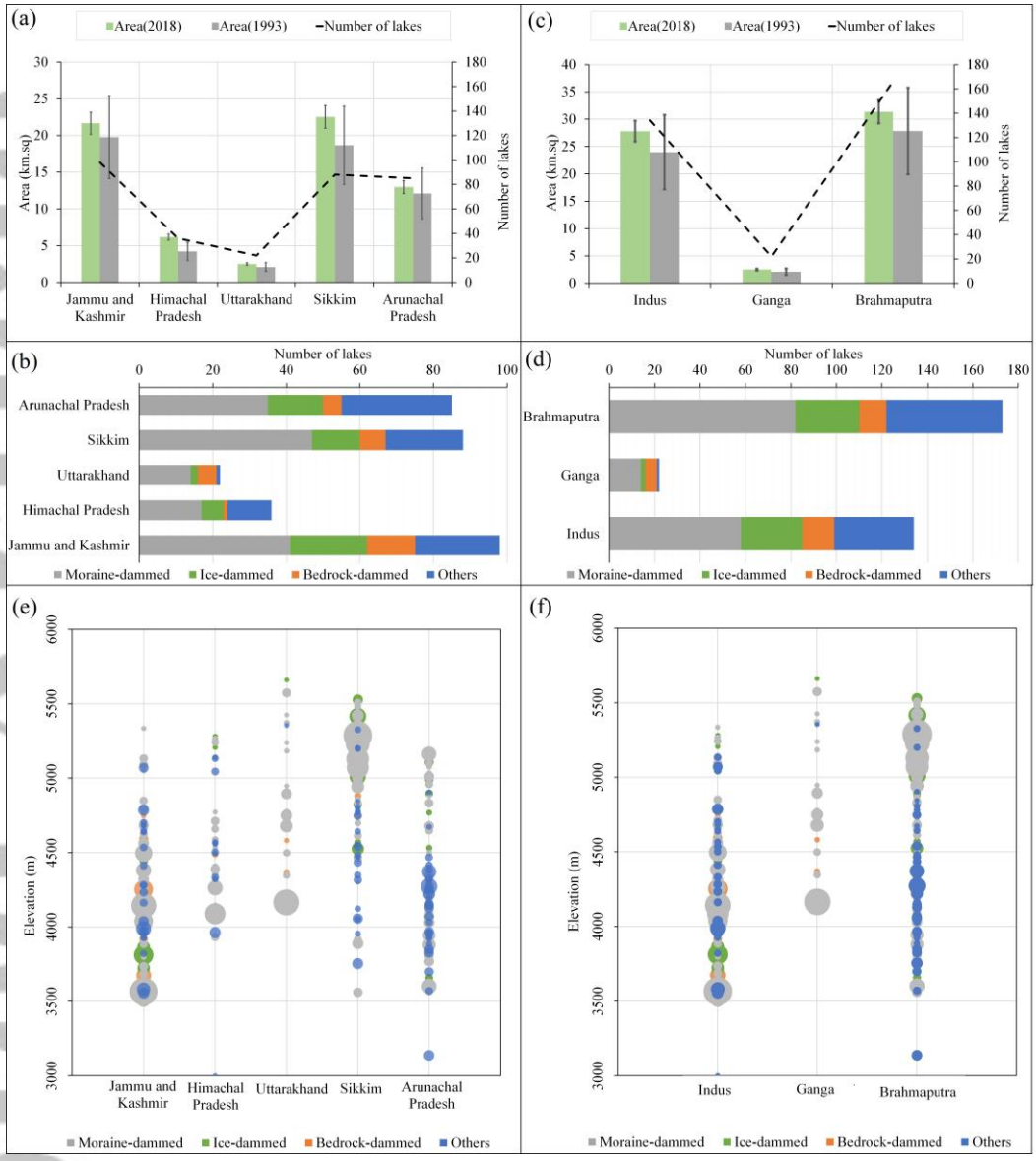

Figure 3. Areal distribution of lakes in various states (a) and basins (c). The dotted line is plotted in correspondence with the secondary axis to represent the number of lakes. Distribution of various lake types in states (b) and basins (d). Figures (e) and (f) represent glacial lakes in various elevation zones, the colour of the circles represent various lake types, whereas the size of the circles represents the size of the lake.

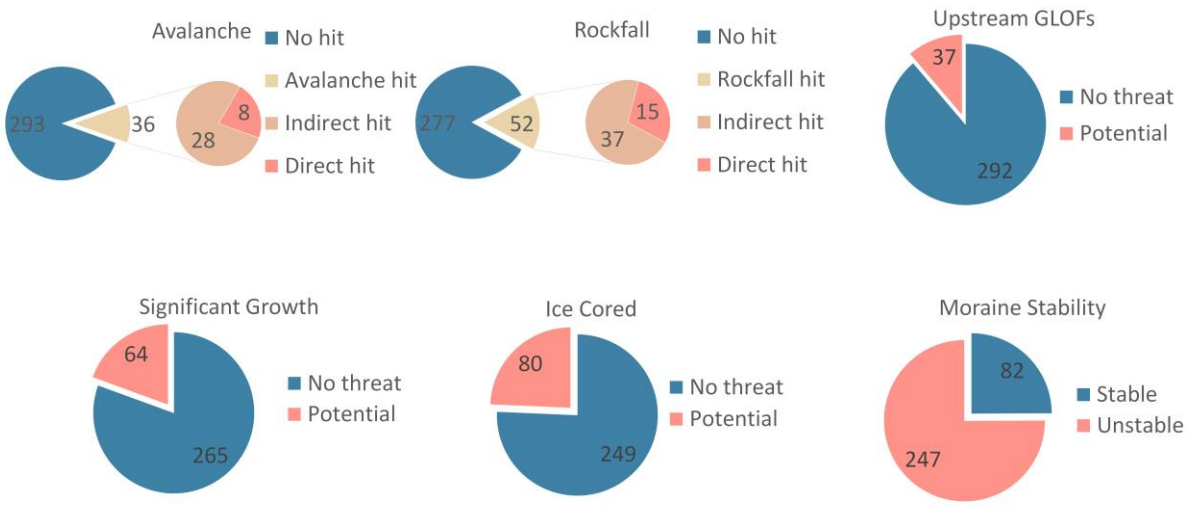

Figure 4. Summary of hazard parameters.

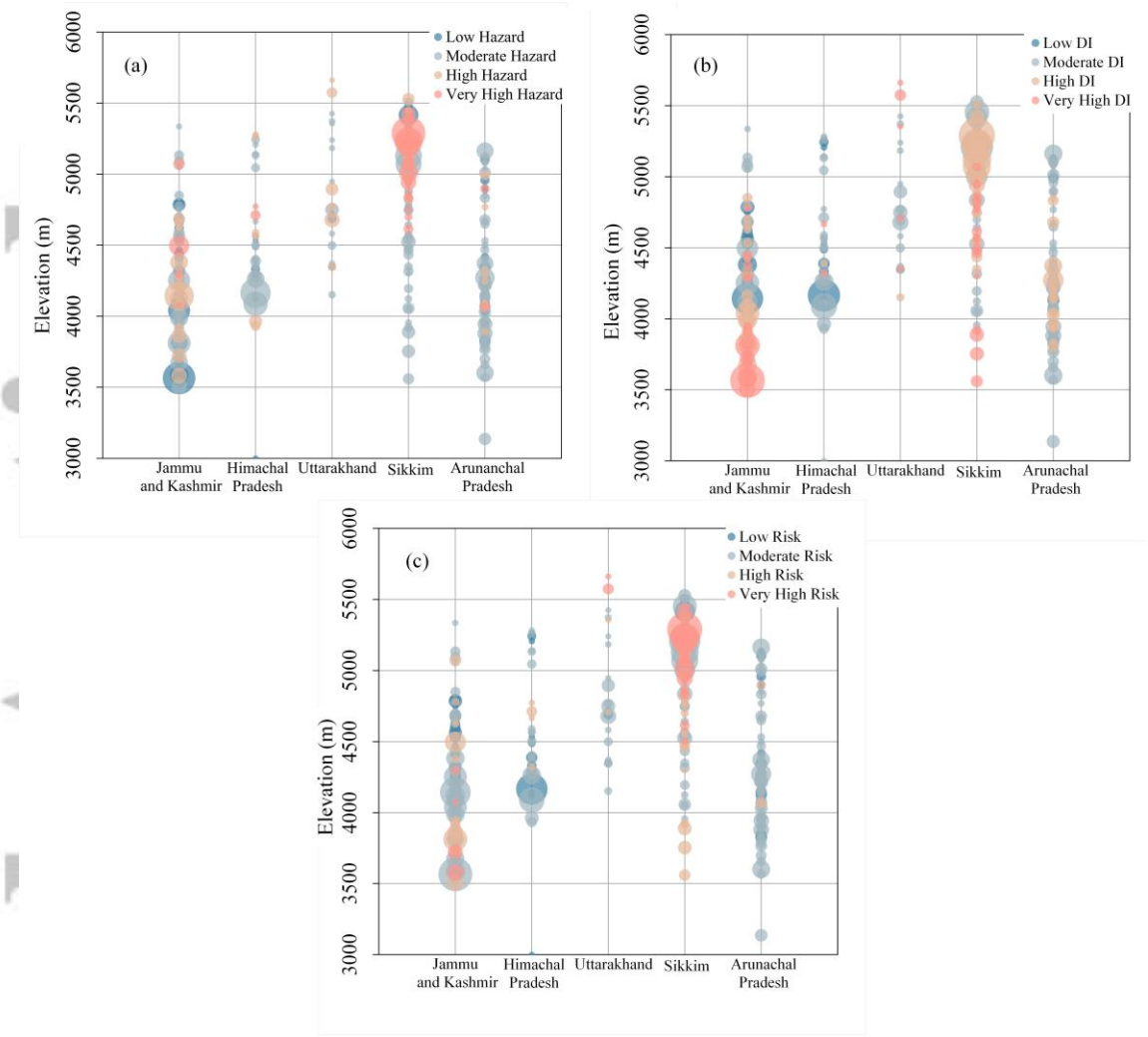

Figure 5. Distribution of (a) hazard, (b) downstream impact (DI) and (c) risk in various elevation zones. Colour of the circle represents very high, high, moderate and low rankings of risk, hazard and downstream impact. The size of the circle represents the size of the lake.

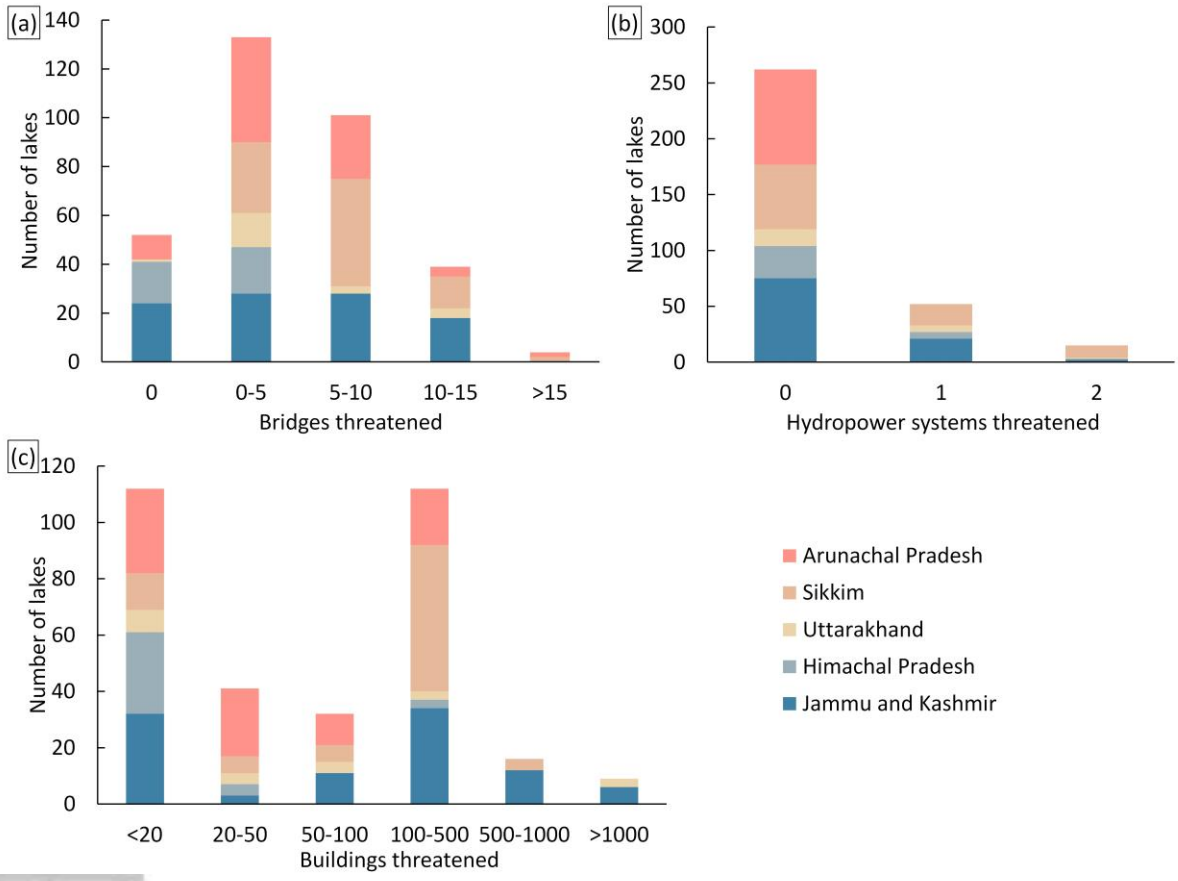

Figure 6. Downstream impact summary representing the potential number of (a) bridges, (b) hydropower systems and (c) buildings threatened by GLOFs

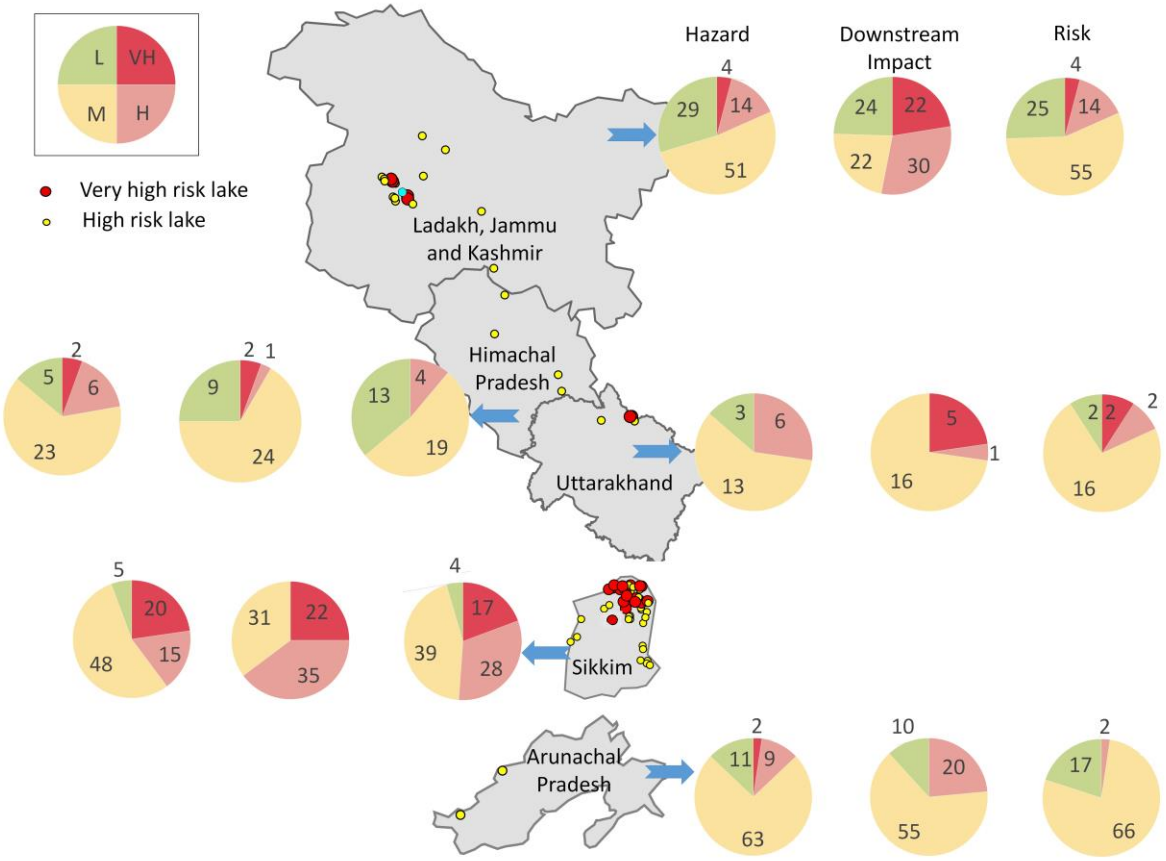

Figure 7. Distribution of hazard, downstream impact and risk classification (pie charts) for various states.

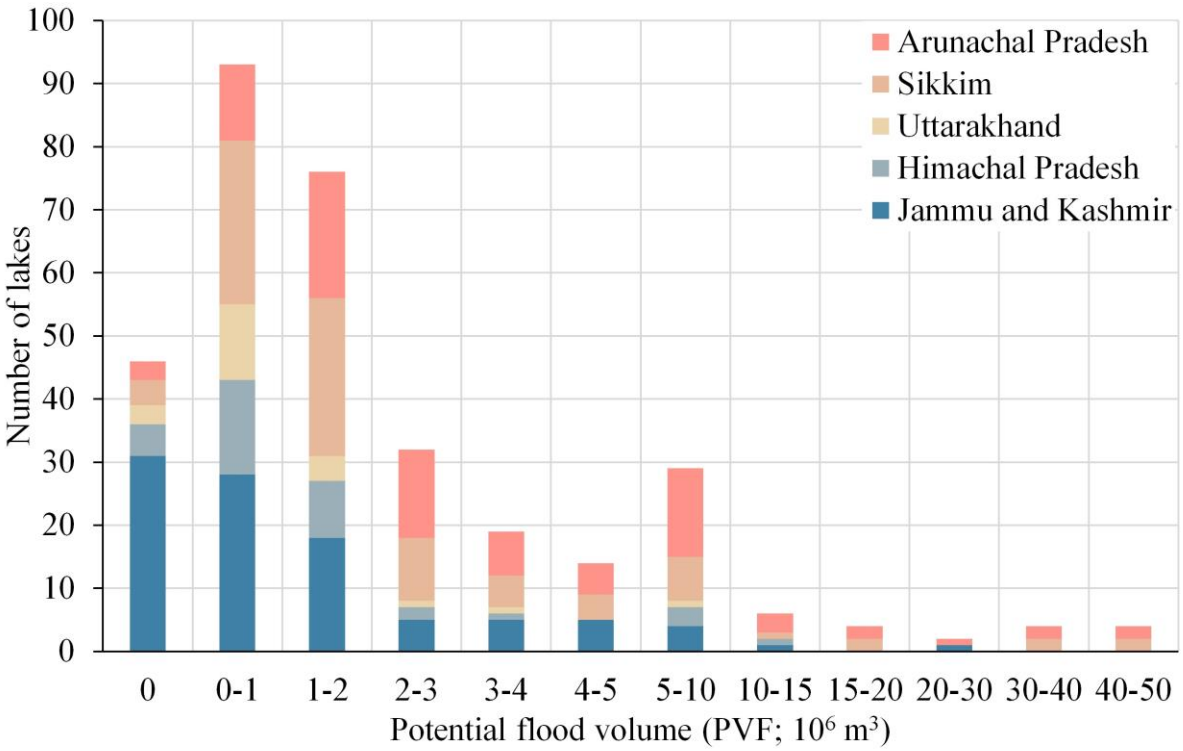

Figure 8. Distribution of PFV for the lakes in Indian Himalayas.

Table 1. Lake details, hazard, downstream impact, risk ranking and PFV of lakes identified as very high-risk lakes. In hazard assessment 1 represent yes and 0 represent no. Ranking of 0 represents low, 1 represents moderate, 2 represents high, and 3 represents very high. Additional details of all the 329 lakes are provided in the supplementary material (Supplementary table sheet 1)

		Lake details						Hazard						Downstream impact			Ranking			
Lake Id this study	**Other studies**	**Longitude (°)**	**Latitude (°)**	**Elevation (m)**	**Aspect (°)**	**Area (km^2) 1993**	**Area (km^2) 2018**	**Significant expansion**	**Lakes upstream**	**Presence of ice core**	**Avalanche**	**Rock fall**	**Steep moraine (slope >10°)**	**Buildings**	**Bridges**	**Hydropower systems**	**Hazard raking**	**Downstream impact raking**	**Risk raking**	**PFV (10^6 m^3)**
6		75.373	34.185	4294	35	0.179	0.121	0	0	1	1	0	1	1400	10	1	3	3	3	1.86±0.82
21		75.085	34.391	4074	300	0.051	0.061	0	0	1	1	0	1	200	5	0	3	2	3	0.7±0.31
27		75.058	34.422	3580	280	0.382	0.399	0	0	0	1	0	0	650	7	1	2	3	3	0.11±0.07
34		75.377	34.139	3722	20	0.33	0.334	0	0	1	0	0	1	1000	10	1	2	3	3	0.19±0.08
139		79.487	30.981	5661	30	0.027	0.051	1	0	1	0	1	1	1300	13	1	2	3	3	0.55±0.24
153	4	79.46	30.976	5574	220	0.119	0.177	1	0	1	0	0	1	1300	13	1	2	3	3	3.17±1.4
159	2, 3	88.546	27.993	5178	75	0.562	0.595	0	0	1	1	1	1	350	8	0	3	2	3	8.17±3.6
160	2, 3, 5	88.713	28.005	5231	340	1.155	1.247	1	0	1	1	1	1	300	5	0	3	2	3	49.89±21.95
161	2, 3	88.616	27.975	5010	30	0.574	0.576	0	0	0	1	1	1	350	8	0	3	2	3	16.78±7.38
164		88.657	27.816	4613	90	0.143	0.143	0	0	0	1	0	1	300	10	1	3	3	3	2.34±1.03
173	3	88.789	27.873	4943	160	0.098	0.104	0	0	0	1	0	1	275	8	1	3	3	3	1.49±0.66
174	3	88.509	27.982	4942	200	0.028	0.376	1	0	0	1	1	1	152	11	0	3	2	3	1.8±0.79

176		88.638	27.873	5147	185	0.078	0.086	0	0	0	1	0	1	104	6	0	3	2	3	1.14±0.5
180		88.806	27.854	5068	210	0.09	0.097	0	0	1	0	0	1	275	8	1	2	3	3	1.36±0.6
202	1, 3, 5	88.816	27.99	5288	300	1.647	1.775	0	0	1	1	1	1	150	3	0	3	2	3	19.93±8.77
207		88.761	27.895	5232	280	0.466	0.476	0	1	1	1	0	1	172	8	0	3	2	3	12.78±5.62
209	1, 2	88.561	28.014	5070	110	0.262	0.27	0	0	0	1	1	1	350	8	0	3	2	3	5.06±2.23
214	2	88.639	28.002	5423	350	0.319	0.317	0	0	1	1	1	1	395	8	0	3	2	3	7.21±3.17
218	1	88.863	27.865	4834	200	0.135	0.141	0	0	0	1	1	1	195	8	1	3	3	3	1.76±0.77
225		88.672	27.92	4857	20	0.095	0.097	0	0	0	1	0	1	135	10	0	3	2	3	0.3±0.13
228		88.801	27.993	5284	300	0.095	0.086	0	0	0	1	0	1	223	11	0	3	2	3	0.76±0.33
231	3	88.747	27.864	5089	280	0.117	0.185	1	0	1	1	0	1	135	10	0	3	2	3	0.6±0.26
329		88.514	27.7	4505	210	0.094	0.076	0	0	1	0	0	1	130	16	2	2	3	3	0.12±0.05
* 1: Ives et al., 2010 (ICIMOD), 2: Worni et al., 2013, 3: Aggarwal et al., 2017, 4: Raj & Kumar, 2016, 5: Abdul Hakeem et al., 2018																			

Table 2. Details of lakes having PFV higher than 5 $\times 10^6$ m^3. Ranking value (o) represent low, (1) represent moderate, (2) represent high and (3) represent very high. For hazard (1) represent yes and (0) represent no.

	Lake details							Hazard						Downstream Impact			Ranking			
Lake Id this study	**Common Name**	**Longitude (º)**	**Latitude (º)**	**Elevation (m)**	**Aspect (º)**	**Area (km^2) 1993**	**Area (km^2) 2018**	**Significant expansion**	**Lakes upstream**	**Presence of ice core**	**Avalanche**	**Rockfall**	**Steep moraine (slope> 10º)**	**Buildings**	**Bridges**	**Hydropower systems**	**Hazard raking**	**Downstream impact ranking**	**Risk ranking**	**PFV (10^6 m^3)**
216	Gurudongmar	88.710	28.026	5130	350	1.149	1.12	0	1	0	0	0	1	300	5	0	1	2	1	49.89±21.95
160		88.713	28.005	5231	340	1.155	1.247	1	0	1	1	1	1	300	5	0	3	2	3	49.89±21.95
205	Tso Lhamo	88.756	28.012	5072	340	1.111	1.058	0	0	0	0	0	1	238	14	0	1	2	1	39.54±17.4
206		88.698	28.007	5228	20	0.906	1.018	1	0	1	0	1	1	283	16	0	2	2	2	37.46±16.48
47	J R B lake	75.179	34.666	4252	35	0.746	0.757	0	0	0	0	0	1	78	6	0	1	1	1	24.64±10.84
202	Khangchung Tso	88.816	27.990	5288	300	1.647	1.775	0	0	1	1	1	1	150	3	0	3	2	3	19.93±8.77
279		92.033	27.519	4272	10	0.617	0.588	0	0	0	0	0	1	154	13	0	1	2	1	17.26±7.59
161	Shakhocho	88.616	27.975	5010	30	0.574	0.576	0	0	0	1	1	1	350	8	0	3	2	3	16.78±7.38
132	Chandra Tal	77.615	32.483	4262	300	0.53	0.49	0	0	0	0	1	1	48	2	0	1	1	1	13.34±5.87
207		88.761	27.895	5232	280	0.466	0.476	0	1	1	1	0	1	172	8	0	3	2	3	12.78±5.62
299		93.820	28.616	3600	315	0.467	0.468	0	0	0	0	0	1	5	5	0	1	1	1	12.49±5.49
71	Shaushar	75.236	34.991	4142	200	1.296	1.342	0	0	1	0	0	1	0	0	0	2	0	1	9.02±3.97
324	South Lhonak	88.195	27.912	5210	75	0.59	1.44	1	1	1	0	0	1	40	3	0	2	1	1	8.92±3.92
313		93.578	28.576	3879	30	0.396	0.363	0	1	0	0	0	1	16	4	0	1	1	1	8.74±3.85

307		93.437	28.305	3944	355	0.196	0.351	1	0	0	0	0	1	10	3	0	1	1	1	8.31±3.66
24	Lolgul gali	74.892	34.444	3864	350	0.345	0.35	0	0	1	0	0	1	1400	3	0	2	2	2	8.3±3.65
159		88.546	27.993	5178	75	0.562	0.595	0	0	1	1	1	1	350	8	0	3	2	3	8.17±3.6
236		88.512	27.672	4525	70	0.319	0.333	0	0	0	0	0	1	12	5	1	1	1	1	7.71±3.39
48		75.137	34.697	4121	350	0.633	0.549	0	0	1	0	0	1	78	6	0	2	1	1	7.32±3.22
214		88.639	28.002	5423	350	0.319	0.317	0	0	1	1	1	1	395	8	0	3	2	3	7.21±3.17
283		91.875	27.673	4220	20	0.336	0.307	0	0	0	0	0	1	40	11	0	1	1	1	6.89±3.03
133	Geepang gath	77.220	32.525	4088	160	0.42	0.941	1	0	0	0	1	1	3	2	1	1	1	1	6.76±2.97
156		78.987	30.745	4749	330	0.229	0.292	1	0	0	0	0	1	82	0	1	1	1	1	6.42±2.83
282		91.870	27.746	4371	20	0.459	0.439	0	0	0	0	0	1	165	10	0	1	2	1	6.33±2.79
131	Lam Dal	76.332	32.336	3962	320	0.274	0.272	0	0	1	0	0	1	9	4	0	2	1	1	5.82±2.56
196	Tsomgo	88.763	27.375	3753	270	0.231	0.269	0	0	0	0	0	1	275	9	2	1	3	2	5.45±2.4
130		78.167	31.661	4278	20	0.122	0.257	1	0	0	0	1	1	6	0	1	1	1	1	5.36±2.36
310		93.726	28.594	4218	260	0.252	0.25	0	0	0	0	0	1	16	4	0	1	1	1	5.14±2.26
311		93.712	28.585	3894	20	0.135	0.144	0	1	0	0	0	1	16	4	0	1	1	1	5.14±2.26
209		88.561	28.014	5070	110	0.262	0.27	0	0	0	1	1	1	350	8	0	3	2	3	5.06±2.23
210		88.572	28.007	4997	130	0.275	0.268	0	1	0	0	1	1	350	8	0	1	2	1	5.06±2.23
81		74.961	35.082	4320	0	0.251	0.246	0	1	0	0	0	1	135	11	0	1	2	1	5.03±2.21